A dietary flavone confers communicable protection against colitis through NLRP6 signaling independently of inflammasome activation

Katarina Radulovic, Sylvain Normand, Ateequr Rehman, Anne Delanoye-Crespin, J Chatagnon, Myriam Delacre, Nadine Waldschmitt, Lionel F Poulin, Juan Iovanna, Bernhard Ryffel, et al.

▶ **To cite this version:**

Katarina Radulovic, Sylvain Normand, Ateequr Rehman, Anne Delanoye-Crespin, J Chatagnon, et al.. A dietary flavone confers communicable protection against colitis through NLRP6 signaling independently of inflammasome activation. Mucosal Immunology, 2017, 11 (3), pp.811-819. 10.1038/mi.2017.87 . hal-01788846

HAL Id: hal-01788846
https://hal.science/hal-01788846v1

Submitted on 17 May 2018

HAL is a multi-disciplinary open access archive for the deposit and dissemination of scientific research documents, whether they are published or not. The documents may come from teaching and research institutions in France or abroad, or from public or private research centers.

L'archive ouverte pluridisciplinaire **HAL**, est destinée au dépôt et à la diffusion de documents scientifiques de niveau recherche, publiés ou non, émanant des établissements d'enseignement et de recherche français ou étrangers, des laboratoires publics ou privés.

A dietary flavone confers communicable protection against colitis through NLRP6 signaling independently of inflammasome activation.

Authors: K. Radulovic[a,b†], S. Normand[a,†], A. Rehman[c,†], A. Delanoye-Crespin[a], J Chatagnon[a], M Delacre[a], N. Waldschmitt[a], LF. Poulin[a], J. Iovanna[d], B. Ryffel[e], P. Rosenstiel[c], M. Chamaillard[a].

Affiliations:

[a]Univ. Lille, CNRS, Inserm, CHRU Lille, Institut Pasteur de Lille, U1019 - UMR 8204 - CIIL - Centre d'Infection et d'Immunité de Lille, F-59000 Lille, France.

[b]University Hospital Basel, Department of Biomedicine, 4031 Basel, Switzerland.

[c]Institute of Clinical Molecular Biology, Christian-Albrechts-University and University Hospital Schleswig-Holstein, Campus Kiel, 24105 Kiel, Germany.

[d]Centre de Recherche en Cancérologie de Marseille, Inserm U1068, CNRS UMR 7258, Aix-Marseille Université and Institut Paoli-Calmettes, Parc Scientifique et Technologique de Luminy, Marseille, France.

[e]CNRS UMR 7203, Paris, France.

Correspondence should be addressed to: Mathias Chamaillard, PhD, Phone number: +33359317427, Fax number: +33359317480, E-mail: mathias.chamaillard@inserm.fr.

† These authors shared first authorship.

Running title (56 characters): Apigenin regulates bacterial ecology by Nlrp6 signaling.

Manuscript information: Text pages: 24; Figures: 7 ; Supplementary Figure : 6.

Word count (counting spaces): Title: 131 characters; Abstract: 219 words; Text (excluding Abstract, References, Tables and Figures): 3475 words; References: 30.

Key words: colitis, flavone, gut microbiota, inflammasome.

Conflict of interest: None to be declared.

Abstract.

The flavone is a class of polyphenols that are found in many plant-derived food sources. Herein, we provide evidence that the anti-inflammatory and anti-proliferative effect of the flavone apigenin relies on the regulation of the gut microbiota by the NOD-like receptor family pyrin domain containing 6 (Nlrp6). We find that the anti-proliferative effect of apigenin and subsequently its protective effect against colitis were dominantly transmitted after co-housing, while being compromised in mice that are deficient in Nlrp6 within the same facility. Sequencing of the 16S ribosomal RNA revealed a shift in the composition of the gut microbiota in apigenin-treated mice that was not observed in the absence of Nlrp6. In response to injury, no protective effect of apigenin was observed in the absence of the downstream c-type lectin Reg3b that is regulated by Nlrp6 signaling in the colon. In contrast, loss of either caspase-1 or its adaptor protein ASC failed to abrogate the protective effect of apigenin against colitis. Collectively, these data indicate that apigenin modulated an inflammasome-independent mechanism in which Nlrp6 shapes a specific configuration of the gut microbiota for protecting mice against colitis. Our study highlights that an intact Nlrp6 signaling pathway is modulated in response to a prominent constituent of the human diet which may point toward improved ways to define and treat inflammatory bowel diseases.

Introduction

The gut is inhabited by the microbiota that consists of highly diverse bacterial microorganisms with widely differing living requirements. Notably, the genome of the trillions of bacteria residing in the gut (commonly referred as the intestinal microbiome) encompasses several biosynthetic pathways that are primarily influenced by drug intake, hygiene and nutrition. One can consider the microbiota as our “extended self”, in as much as this multicellular organ consumes, stores and redistributes energy harvested from nutrients from the earliest days of life onwards [1]. Throughout the host's entire life, this paradigm is also well exemplified by the beneficial impact of some bacteria on post-natal maturation of the immune system. With this reductionist organ centered-view in mind, symbiosis is defined as an association between organisms of two different species in which each is benefited. Conversely, instability in the composition of gut microbial communities (referred to as dysbiosis) has been linked to greater intestinal permeability in several common human illnesses with increasing socio-economic impacts, such as inflammatory bowel diseases. In particular, Crohn’s disease is associated with a greater preponderance of certain Bacteroidetes and a lower abundance of Firmicutes [2, 3]. However, it remains elusive how to restore symbiotic host-microbiota interactions in Crohn’s disease patients.

Herbal-based supplements are used for many years as nutraceuticals for the treatment of various symptoms related to inflammatory responses such as pain, headache and diarrhea. Among nutraceuticals, dietary flavonoids are the largest class of polyphenols that have been known as pigments for over a

century (named from the latin word *flavus* meaning yellow). Besides their role in plant pigmentation and flavor, their common structure is a skeleton of diphenylpropane that confers a diversity of biochemical functions on plant physiology, including seed maturation, dormancy and protection from oxidative stress, UV radiation, phytopathogens and herbivores. Meanwhile, a plethora of epidemiological studies indicated that diets rich in some subclasses of dietary flavonoids are largely responsible for overall metabolic and cardiovascular health of humans [4-7]. Notably, a lower risk of prostate cancer in men and of breast cancers in postmenopausal women was associated with intake of soy isoflavones and of apigenin (4′,5,7-trihydroxyflavone) as what observed for the lowered risk of colorectal cancer among individuals who regularly drink green tea [8]. Conversely, an enhanced risk of colorectal cancer is associated with low intake of flavonoids [8]. Furthermore, supplementation of the diet with the flavone apigenin was also found to act on intestinal homeostasis, as it exerted protective effects in several preclinical models of colitis [9-11]. Apigenin is a widely distributed secondary metabolite throughout the plant kingdom with a 2-phenylchromen-4-one (2-phenyl-1-benzopyran-4-one) backbone, representing an aglycone of several naturally occurring plant glycosides. The pharmacological properties of apigenin include oxidative effects, which may result in senescence and in wound healing [12]. Nevertheless, it remain poorly understood how the apigenin exerts its anti-inflammatory effect apart from its direct radical scavenging properties. Herein, we provide evidence that it could modulate the composition of the gut microbiota through the NOD-like receptor family pyrin domain containing 6 (Nlrp6) protein protecting mice from colitis.

Results

Apigenin protects mice from colitis

The physicochemical properties relevant to human health of apigenin are primarily determined by its absorbability from ingested food. To overcome this issue, we assessed the potential effect of intraperitoneal administration of apigenin on the resolution of inflammation. To this end, we made use of a preclinical model of colitis that is induced by administration in the drinking water of dextran sodium sulphate (DSS) for 7 days. This sulphated polysaccharide is known to promote epithelial tissue disruption, which leads to microbial translocation and increased secretion of key signals of the acute phase response by infiltrating inflammatory cells. As expected, about 15% decrease of the initial body weight was observed in wild-type mice at nine days after DSS administration (Fig. 1A). In contrast, an improved body weight loss was noticed in mice that received apigenin together with a significantly lowered disease-activity index (Fig. 1A, B) and shortening of their colon (Fig. 1C). Consequently, histological examination of the haematoxylin and eosin-stained sections of the colon revealed a markedly reduced severity of colitis in apigenin-treated mice when compared to controls as illustrated by erosion of the colonic crypts and massive infiltration of inflammatory cells (Fig. 1D, E). Collectively, preventive administration of apigenin was found to improve signs of colitis in the wild-type setting as what was observed with other flavones [13].

Co-housing experiments revealed that the anti-inflammatory effect of apigenin is communicable to adult wild-type mice.

To assess whether the gut microbiota may contribute to the protective effect of apigenin against colitis, non-treated and apigenin-treated mice were cohabitated for 3 weeks before DSS challenge and disease activity was daily monitored. As what observed among single-housed treated mice, the body weight loss (Fig. 2A) and disease activity index (Fig. 2B) were improved among non-treated animals that were co-housed with the apigenin treated one (referred herein as ch-*WT*). Consequently, colon length shortening was reduced among ch-*WT* mice (Fig. 2C), while simultaneously mitigating histological scores (Fig. 2D, E). Collectively, co-housing experiment revealed that the protective effect of apigenin against colitis was communicable, suggesting that apigenin may protect the mucosa from overwhelming inflammation by regulating the composition of the gut microbiota rather than by any direct anti-inflammatory effects.

Apigenin treatment alters the composition of the gut microbiota through an intact Nlrp6 signaling pathway.

By 16S rRNA gene sequencing and subsequent phylogenetic analyses, we next addressed whether the anti-inflammatory role of apigenin was associated with alterations in the bacterial composition of the gut microbiota. Statistical Analysis Of SIMilarity (ANOSIM) on Jaccard distances revealed that the gut microbiota composition of apigenin-treated *WT* mice was markedly different from the one of controls ($R^2 = 0.33$, $p = 0.015$; Fig. 3A). A Lefse analysis revealed an expansion of several bacterial taxa derived from Bacteroidetes group, including *Rikenellaceae*, *Bacteroidales* and *Bacteroides*, among apigenin-treated mice. Furthermore, apigenin treatment in wild-type

mice led to a reduction of bacterial operational taxonomic units derived from *Clostridium* and *Lachnospiraceae* (Fig. 3B). Equally of importance, the bacterial communities among co-housed mice were found similar as determined by PcoA and analysis of similarity (p=0.1515). This result suggests that the apigenin-induced changes in the gut microbiota harbors dominance upon co-housing as a likely consequence of coprophagy (Supplementary Fig. 2). In addition, a trend of higher bacterial diversity and richness was observed in the feces collected from animals treated with apigenin in comparison to non-apigenin treated animals (Supplementary Fig. 3). To obtain further insights how apigenin impacts on the composition of the gut microbiota, we performed additional 16S rRNA gene sequencing analysis of feces from mice that are deficient for Nlrp6 that is known to control gut bacterial ecology (Supplementary figure 1A). In line with previous findings [14-16], large-scale changes in the gut microbiota composition gave rise to a reduced bacterial diversity in the absence of Nlrp6 ($p = 0.001$; Supplementary figure 1B). Notably, the gut bacterial ecology of *Nlrp6*-deficient mice was characterized by a lowered abundance of non-flagellated and butyrate-producing bacteria belonging to the Bacteroidetes phylum (including *Alistipes*, *Barnesiella* and *Allobaculum*), which was correlated with an outgrowth of unclassified *Porphyromonadaceae* and Clostridiales genera (Supplementary Fig. 1C). In contrast to what was observed in wild-type mice, we failed to notice major global changes in the composition of the gut microbiota from apigenin-treated and untreated *Nlrp6*-deficient mice (ANOSIM, $p = 0.283$; Fig. 3A). Collectively, the impact of apigenin on the gut microbiota was dependent

on Nlrp6 expression and associated with its anti-inflammatory effect that can be acquired *de novo* after cohousing.

The anti-inflammatory effect of apigenin relies on an intact Nlrp6 signaling pathway independently of caspase-1 and its adaptor ASC.

Even if the disease risk in mice deficient for Caspase-1 (encoded by the *Casp1* gene) is similar to that observed in the absence of the Nlrp6 protein (8), it is still not clear whether Nlrp6 may physiologically form a molecular platform with caspase-1 and the apoptosis-associated speck-like protein containing a caspase-recruitment domain (namely Asc encoded by *Pycard* gene). In this context, we next determined whether apigenin may protect against DSS-induced colitis through Caspase-1. To this end, caspase-1-deficient (*Casp1*$^{-/-}$) mice were subjected to DSS as previously described. About 17% of initial body weight of *Casp1*$^{-/-}$ mice was lost at day 9 (Fig. 4A), whereas apigenin significantly reduced body weight loss (Fig. 4A) and colon length shortening (Fig. 4B) as what observed in apigenin-treated wild-type animals (Fig. 1). To verify these results, we evaluated the efficacy of apigenin in mice that are deficient for Asc. Consistent with the results observed with *Casp1*$^{-/-}$ mice, disease severity was improved in apigenin-treated *Pycard*$^{-/-}$ mice when compared to untreated mutant animals (Fig. 4E,F). Consistently, histological investigation showed reduced infiltration of inflammatory cells in apigenin-treated mice that are deficient for either Caspase-1 (Fig. 4C, D) or Asc (Fig. 4G, H). In contrast, experiments with *Nlrp6*-deficient mice failed to reveal any differences in protection from colitis between apigenin-treated and non-treated animals as determined by quantifying body weight loss (Fig. 4E),

colon length (Fig. 4F) and the inflammatory response in subsequent histological analysis (Fig. 4G, H). Likewise, apigenin treatment failed to improve wasting disease (Fig. 5A) and colon length shortening (Fig. 5B) in co-housed mice lacking Nlrp6. Consequently, histological scores were not improved in the absence of Nlrp6 as evidenced by both crypt erosion and massive infiltration of inflammatory cells within colons of either non-treated single-housed or co-housed *Nlrp6*-deficient mice (Fig. 5C, D), indicating that the modulation by apigenin of the Nlrp6 signaling pathway is independent of housing conditions. Collectively, Nlrp6 determines to a large extent how apigenin protects mice from intestinal inflammation by modulating the composition of the gut microbiota independently of inflammasome activation as what observed in response to several enteric viruses [17].

An intact Nlrp6 pathway is required for the anti-proliferative effect of apigenin on intestinal epithelial cells.

We next evaluated if the changes in the gut microbiota in response to apigenin may impact intestinal homeostasis by qRTPCR analysis on the colon from control mice that were either single-housed or co-housed with apigenin-treated animals. The impact of apigenin on the gut microbiota suffices to enhance the expression of Nlrp6 as a potential first signal (Fig. 6A). Given the properties of apigenin on cell cycle, we next examined the impact of apigenin on the proliferative index of the epithelium by staining the colonic sections for Ki67. In line with previous findings, imunohistochemical analysis using Ki67 revealed a lower number of proliferating epithelial cells in the colon of apigenin-treated wild-type mice when compared to control animals (Fig. 6B,

C), yet the number of cleaved caspase-3-positive cells was found similar (Supplementary Fig. 4). Furthermore, a greater phosphorylation of Akt and of Signal transducer and activator of transcription 3 (STAT3) was observed in the colon of either untreated wild-type or mutant mice when co-housed with mice that were treated with apigenin (Supplementary Fig. 5). In contrast, the anti-proliferative effect of apigenin was abrogated in mice that are deficient for Nlrp6 (Fig. 6B, C). Of note, the reduced proliferation index of apigenin-treated mice was dominantly transmitted after co-housing of control animals but not *Nlrp6*$^{-/-}$ mice (Fig. 6C). These results suggested us that apigenin may modulate several mitogenic factors that are secreted downstream of the Nlrp6 signaling pathway. To test this hypothesis, we evaluated the efficacy of apigenin for protecting against colitis in mice that are deficient for the stress-induced regenerating islet-derived protein 3 b (Reg3b). Reg3b is a c mitogenic -type lectin which expression is lowered in the colon of *Nlrp6*$^{-/-}$ mice (Supplementary Fig. 6). In line with our previous findings, Reg3b was important in attenuating the colonic inflammatory reponse to DSS (Figure 7), providing a mechanism how alterations in the bacterial composition of the gut microbiota by apigenin could specifically lower the proliferation rate of epithelial cells and subsequently protect mice.

Discussion

Apigenin is a secondary metabolite of flavonoids from photosynthetic plants that has been propagated as a natural remedy for protection against several diseases and ailments. Whereas apigenin exerts direct oxidative effects and antibacterial killing activity [18], our results reveal an unexpected mode of action, which relies on compositional changes in the gut microbiota downstream of the Nlrp6 signaling pathway, deregulation of which has been shown to confer risk of colitis [14]. Understanding this paradigm is of importance as the dysbiotic microbiota of *Nlrp6*-deficient mice contributes to their metabolic syndrome [19]. Notably, the lowered proliferation rate of intestinal epithelial cells in response to the apigenin-induced shift in the composition of the gut microbiota merits further study as it may contribute to the persistence of the microbiome configuration driven by post-dieting weight regain [20]. Co-housing experiments revealed a dominant horizontal transmission of the anti-inflammatory properties of apigenin that likely depends on the coprophagic and grooming behaviors of mice. Of note, a lowered microbial diversity of the gut microbiota is observed in most patients with inflammatory bowel diseases which may contribute to the heterogeneous efficacy of flavonoids in inflammatory bowel diseases [21]. Meanwhile, the differences in the gut bacterial ecology of *Nlrp6*-deficient mice coincided with a lowered expression of the c-type lectin Reg3b and conferred their resistance to the anti-proliferative and anti-inflammatory effect of the aforementioned phytosterol. However, the efficacy of apigenin was not compromised by the dysbiotic microbiota of *Casp1*- and *Pycard*-deficient mice even if their disease risk is similar to that observed in the absence of the Nlrp6 protein [14]. On this basis,

our study revealed an inflammasome-independent mechanism whereby the protective effect of apigenin relies on Nlrp6 signaling and its downstream effectors, including the c-type lectin Reg3b and potentially some antimicrobial peptides that are also regulated by Nlrp6 [22]. Equally interesting is the need to define whether the anti-inflammatory effect of apigenin may rely on the regulation of cholesterol metabolism [23, 24]. Of note, the compositional change in the microbiota of *Nlrp6*-deficient mice results in a low taurine and high spermine/histamine levels which contributes to its dominant takeover [22]. Alternatively, one may hypothesize that apigenin may promote a growth advantage of several bile-tolerant members of the *Alistispes* genus that were found less abundant in the absence of Nlrp6. Collectively, our study demonstrates that the protective therapeutic action of a common dietary flavone on intestinal inflammation depend on the NOD-like receptor Nlrp6 and on subsequent secretion of the c-type lectin Reg3b. The effect is independent of the classical inflammasome function mediated via caspase-1, but involves preservation of epithelial barrier integrity and an altered composition of the gut microbiota.

Methods

Mice. All animal studies were approved by the local investigational review board (CEEA232009R) in an accredited establishment (N° B59-108) according to governmental guidelines N°86/609/CEE. Age- and gender-matched Nlrp6-deficient (*Nlrp6*$^{-/-}$), Caspase 1-deficient (*Casp1*$^{-/-}$), Asc-deficient (*Pycard*$^{-/-}$), *Reg3b*-deficient (*Reg3b*$^{-/-}$) and control C57BL6/J mice had free access to a standard laboratory chow diet in a half-day light cycle exposure and temperature-controlled environment. Colitis was induced by giving mice 2% (W/v) DSS (TdB Consultancy) for a period of seven days followed by drinking water for two to three days. DSS was dissolved in autoclaved drinking water. Signs of morbidity, including body weight, stool consistency and occult blood or the presence of macroscopic rectal bleeding gross, were monitored daily as previously described [25]. Apigenin (25 µg/mouse; Santa Cruz) was given intraperitoneally twice a week for one to three weeks before the induction of colitis. For co-housing experiments, mice were kept in the same cage for a period of 3 weeks before exposure to DSS and left together during colitis. At the end of the challenge, mice were autopsied to assess the severity of the disease by measurement of colon lengths and by histological scoring. At one cm above the anal canal, a resection specimen of the distal colon was dissected out and kept frozen in RNAlater until subsequent RNA isolation and qRTPCR analyses. Tissue specimens were collected and kept frozen until further quantification of transcript and protein levels. One piece of colon was fixed in 4% paraformaldehyde and embedded in paraffin for immunohistochemistry analysis by two investigators.

Histological scoring and immunohistochemistry. Histological scoring of hematoxylin and eosin (H&E) stained sections take into account the level of inflammatory cells infiltration and the epithelial damage as previously described [25]. Intestinal tissue was fixed in formalin, dehydrated in series of increasing concentration of alcohols and toluene before being embedded in paraffin. For immunohistochemistry, 5 µm-thick tissue sections were placed on Superfrost Plus slides (Thermo Scientific), incubated for 10 min at 60° C and rehydrated through a series of graded alcohols and distilled water. Endogenous peroxidases were blocked by 3% hydrogen peroxide for 10 min. Antigen retrieval was performed in citrate buffer (10 mM, pH 6) by steaming sections in a microwave oven for 20 min. Tissue sections were blocked with 5% BSA/PBS for 30 min at RT and primary Ab against either Ki67 (1:100, ab15580, Abcam) or cleaved caspase3 (1:50, 9661, Cell Signalling) was directly applied and incubated one hour at room temperature (RT) or overnight at 4°C, respectively. Slides were washed 3x in PBS before applying secondary peroxidase-conjugated goat anti-rabbit IgG (1:100, Interchim) Ab two hours at RT. Targeted antigens were visualized by using 3.3'-diaminobenzidine solution (BD Pharmingen) followed by nuclear counterstain with hematoxylin. Ki67+ and cleaved caspase3+ cells were counted in all intact crypts of each section.

ELISA. Protein levels of IL-1b were determined from the supernatants of colon homogenates by specific ELISA according to the manufacturer's instructions (R&D system).

Microbiota analysis. 16S rRNA gene variable region V3 and V4 was amplified using dual indexed fusion primers, in brief primers consist of illumina

linker sequence, 12 base barcode sequence and heterogeneity spacer followed by either 16S rRNA gene specific forward (319F: ACTCCTACGGGAGGCAGCAG) or reverse (806R: GGACTACHVGGGTWTCTAAT) primer sequences [26]. DNA was amplified using above mentioned composite primers in duplicate in a GeneAmp PCR system 9700 (Applied Biosystems, Foster City, California, USA) using the following cycling conditions: an initial denaturation of 3 min at 98°C followed by 30 cycles, denaturation at 98°C for 10 seconds, annealing at 50°C for 30 seconds and elongation at 72°C for 30 seconds. Final extension was at 72°C for 10 minutes. Amplified product was run on agarose gel to assess the amplicon size and amplification performance. Amplicons quantities were normalized using SequalPrep kit (Invitrogen) and pooled as a single library. Sequencing was performed using Illumina MiSeq using 2 x 300 sequencing kit with standard HP10 and HP11 primers. Sequencing reads were primarily processed for quality control using the software MOTHUR. Forward and reverse reads were assembled to form contigs, reads not having perfectly matched specific primers and barcodes, having any ambiguous base and more than 8 homopolymers were removed from downstream analysis. Sequences not aligning to desired bacterial V3-V4 variable regions, suspected chimera and likely to be of non-bacterial origin were detected and removed. Sequences with at least 97% similarity were clustered in into Operational Taxonomical Units (OTUs). These OTUs were classified taxonomically using Mothur modified Greengenes reference and taxonomy database [27]. Principle coordinate analysis (PcoA) was performed on Jaccard distances among communities. Principle coordinates were visualized using rgl

with in R application package (www.r-project.org). Linear Discriminant Analysis (LDA) with Effect Size (LEfSe) was implemented to identify OTUs differentially enriched or deleted in apigenin treated and untreated animals [28]. LEfSe Analysis was performed in Mothur using 1000 bootstrap iteration for LDA score calculation. Observed number of phylotypes, Shannon index, non-parametric estimate of Shannon diversity index, and Chao1 richness and phylodiversity were calculated within Mothur as parameters of alpha diversity indices in apigenin treated and untreated wild type animals.

Gene expression and western-blotting analysis. Isolated RNA was reverse-transcribed with the cDNA synthesis kit (Agilent Technologies), according to the manufacturer's instructions. The resulting cDNA (equivalent to 500 ng of total RNA) was amplified using the SYBR Green real-time PCR kit and detected on a Stratagene Mx3005P (Agilent Technologies). qRT-PCR was performed using following forward and reverse primers (sequences available upon request). On completion of the PCR amplification, a DNA melting curve analysis was carried out in order to confirm the presence of a single amplicon. *Actb* was used as an internal reference gene in order to normalize the transcript levels. Relative mRNA levels (2-DDCt) were determined by comparing (a) the PCR cycle thresholds (Ct) for the gene of interest and *Actb* (DCt) and (b) DCt values for treated and control groups (DDCt). Proteins for western-blotting were isolated by lysing the colonic tissue in Ripa buffer (10mM Tris-HCl, 150mM NaCl, 1% (v/v) Triton X-100, 0.1% (w/v) SDS, 0.5% (w/v) Na-deoxycholate) supplemented with complete protease inhibitors (Roche). Protein concentration was measured by Pierce

BCA kit (Thermo Fisher) and 10 µg of proteins were loaded and separated by Laemmli 10% SDS-polyacrylamide gel before being transferred onto nitrocellulose membranes. Equal protein loading was verified by Ponceau red staining before blocking the membranes in PBS, 0.05% Tween20, 5% non-fat dry milk. The appropriate primary antibody rabbit anti-βActin (Interchim), rabbit anti-phospho STAT3 (Cell Signalling) and rabbit anti-Akt (CellSignalling). Peroxidase-conjugated goat anti-rabbit IgG Ab (Interchim) was used as secondary Abs (dilutions available upon request).

Statistics. Data were analysed using Prism4.0 (GraphPad Software, San Diego, CA). The non-parametric Kruskal-Wallis test with Dunn's multiple comparison test, the non-parametric Mann-Whitney test or the non-parametric two-way ANOVA test with Bonferroni's multiple comparison test were used. Values represent the mean of normalized data +/- SEM. Asterisk, significant difference $P \leq 0.05$.

Acknowledgments: This work was supported by grants from the Fondation pour la Recherche Médicale (DEQ20130326475). SN was a recipient of a post-doctoral fellowship from the Ligue contre le Cancer. NW was a recipient of a postdoctoral fellowship from Agence Nationale de la Recherche (ANR-13-BSV3-0014-01). PR was supported by the Cluster of Excellence Inflammation at Interfaces, RTG1743 (TP5) and the SFB877 (B9). We thank K. Jambou, C. Bertrand, T. Grandjean, C. Bondu, M. Nesterenko and B. Duchêne for excellent technical assistance.

Authors' contribution. K.R. and S.N. performed the majority of the experimental procedures. A.R. and P.R. contributed to the microbiota analysis. A.D-C. contributed to cell culture experiments and H&E staining and M.D. performed qRT-PCR analysis. N.W. contributed to Ki67 staining. All authors contributed to interpretation of raw data and critically reviewed and/or modified the manuscript. M.C. conceived, designed and wrote the paper.

References

1. Ley RE, Hamady M, Lozupone C, Turnbaugh PJ, Ramey RR, Bircher JS *et al.* Evolution of mammals and their gut microbes. *Science* 2008; **320**(5883)**:** 1647-1651.

2. Scanlan PD, Shanahan F, O'Mahony C, Marchesi JR. Culture-independent analyses of temporal variation of the dominant fecal microbiota and targeted bacterial subgroups in Crohn's disease. *Journal of clinical microbiology* 2006; **44**(11)**:** 3980-3988.

3. Manichanh C, Rigottier-Gois L, Bonnaud E, Gloux K, Pelletier E, Frangeul L *et al.* Reduced diversity of faecal microbiota in Crohn's disease revealed by a metagenomic approach. *Gut* 2006; **55**(2)**:** 205-211.

4. Gonzalez R, Ballester I, Lopez-Posadas R, Suarez MD, Zarzuelo A, Martinez-Augustin O *et al.* Effects of flavonoids and other polyphenols on inflammation. *Crit Rev Food Sci Nutr* 2011; **51**(4)**:** 331-362.

5. Lopez-Posadas R, Ballester I, Mascaraque C, Suarez MD, Zarzuelo A, Martinez-Augustin O *et al.* Flavonoids exert distinct modulatory actions on cyclooxygenase 2 and NF-kappaB in an intestinal epithelial cell line (IEC18). *Br J Pharmacol* 2010; **160**(7)**:** 1714-1726.

6. Seo HS, Ku JM, Choi HS, Woo JK, Jang BH, Go H *et al.* Apigenin induces caspase-dependent apoptosis by inhibiting signal transducer and activator of transcription 3 signaling in HER2-overexpressing SKBR3 breast cancer cells. *Mol Med Rep* 2015; **12**(2)**:** 2977-2984.

7. Xu X, Li M, Chen W, Yu H, Yang Y, Hang L. Apigenin Attenuates Oxidative Injury in ARPE-19 Cells thorough Activation of Nrf2 Pathway. *Oxid Med Cell Longev* 2016; **2016:** 4378461.

8. Hoensch H, Richling E, Kruis W, Kirch W. [Colorectal cancer prevention by flavonoids]. *Medizinische Klinik* 2010; **105**(8)**:** 554-559.

9. Mascaraque C, Gonzalez R, Suarez MD, Zarzuelo A, Sanchez de Medina F, Martinez-Augustin O. Intestinal anti-inflammatory activity of apigenin K in two rat colitis models induced by trinitrobenzenesulfonic acid and dextran sulphate sodium. *Br J Nutr* 2015; **113**(4)**:** 618-626.

10. Marquez-Flores YK, Villegas I, Cardeno A, Rosillo MA, Alarcon-de-la-Lastra C. Apigenin supplementation protects the development of dextran sulfate sodium-induced murine experimental colitis by inhibiting canonical and non-canonical inflammasome signaling pathways. *J Nutr Biochem* 2016; **30:** 143-152.

11. Ganjare AB, Nirmal SA, Patil AN. Use of apigenin from Cordia dichotoma in the treatment of colitis. *Fitoterapia* 2011; **82**(7)**:** 1052-1056.

12. Banerjee K, Mandal M. Oxidative stress triggered by naturally occurring flavone apigenin results in senescence and chemotherapeutic effect in human colorectal cancer cells. *Redox biology* 2015; **5:** 153-162.

13. Shin EK, Kwon HS, Kim YH, Shin HK, Kim JK. Chrysin, a natural flavone, improves murine inflammatory bowel diseases. *Biochemical and biophysical research communications* 2009; **381**(4)**:** 502-507.

14. Elinav E, Strowig T, Kau AL, Henao-Mejia J, Thaiss CA, Booth CJ *et al.* NLRP6 inflammasome regulates colonic microbial ecology and risk for colitis. *Cell* 2011; **145**(5)**:** 745-757.

15. Normand S, Delanoye-Crespin A, Bressenot A, Huot L, Grandjean T, Peyrin-Biroulet L *et al.* Nod-like receptor pyrin domain-containing protein 6 (NLRP6) controls epithelial self-renewal and colorectal carcinogenesis upon injury. *Proceedings of the National Academy of Sciences of the United States of America* 2011; **108**(23)**:** 9601-9606.

16. Chen GY, Liu M, Wang F, Bertin J, Nunez G. A functional role for Nlrp6 in intestinal inflammation and tumorigenesis. *Journal of immunology* 2011; **186**(12)**:** 7187-7194.

17. Wang P, Zhu S, Yang L, Cui S, Pan W, Jackson R *et al.* Nlrp6 regulates intestinal antiviral innate immunity. *Science* 2015; **350**(6262)**:** 826-830.

18. Cushnie TP, Hamilton VE, Lamb AJ. Assessment of the antibacterial activity of selected flavonoids and consideration of discrepancies between previous reports. *Microbiological research* 2003; **158**(4)**:** 281-289.

19. Henao-Mejia J, Elinav E, Jin C, Hao L, Mehal WZ, Strowig T *et al.* Inflammasome-mediated dysbiosis regulates progression of NAFLD and obesity. *Nature* 2012; **482**(7384)**:** 179-185.

20. Thaiss CA, Itav S, Rothschild D, Meijer M, Levy M, Moresi C *et al.* Persistent microbiome alterations modulate the rate of post-dieting weight regain. *Nature* 2016.

21. Ben-Arye E, Goldin E, Wengrower D, Stamper A, Kohn R, Berry E. Wheat grass juice in the treatment of active distal ulcerative colitis: a randomized double-blind placebo-controlled trial. *Scandinavian journal of gastroenterology* 2002; **37**(4)**:** 444-449.

22. Levy M, Thaiss CA, Zeevi D, Dohnalova L, Zilberman-Schapira G, Mahdi JA *et al.* Microbiota-Modulated Metabolites Shape the Intestinal

Microenvironment by Regulating NLRP6 Inflammasome Signaling. *Cell* 2015; **163**(6)**:** 1428-1443.

23. Ren B, Qin W, Wu F, Wang S, Pan C, Wang L *et al.* Apigenin and naringenin regulate glucose and lipid metabolism, and ameliorate vascular dysfunction in type 2 diabetic rats. *European journal of pharmacology* 2016; **773:** 13-23.

24. Jung UJ, Cho YY, Choi MS. Apigenin Ameliorates Dyslipidemia, Hepatic Steatosis and Insulin Resistance by Modulating Metabolic and Transcriptional Profiles in the Liver of High-Fat Diet-Induced Obese Mice. *Nutrients* 2016; **8**(5).

25. Wirtz S, Neufert C, Weigmann B, Neurath MF. Chemically induced mouse models of intestinal inflammation. *Nat Protoc* 2007; **2**(3)**:** 541-546.

26. Fadrosh DW, Ma B, Gajer P, Sengamalay N, Ott S, Brotman RM *et al.* An improved dual-indexing approach for multiplexed 16S rRNA gene sequencing on the Illumina MiSeq platform. *Microbiome* 2014; **2**(1)**:** 6.

27. DeSantis TZ, Hugenholtz P, Larsen N, Rojas M, Brodie EL, Keller K *et al.* Greengenes, a chimera-checked 16S rRNA gene database and workbench compatible with ARB. *Applied and environmental microbiology* 2006; **72**(7)**:** 5069-5072.

28. Segata N, Izard J, Waldron L, Gevers D, Miropolsky L, Garrett WS *et al.* Metagenomic biomarker discovery and explanation. *Genome biology* 2011; **12**(6)**:** R60.

Figure legends:

Figure 1: Apigenin protects mice from colitis. A group of 5 wild-type C57BL6/J mice were intraperitoneally given apigenin at day 7 and 3 prior administration of 2% DSS (w/v) in the drinking water. The body weight loss (A) and disease activity index (B) were daily monitored. At day 9, the colon lengths (C), the representative H&E stained colonic sections (D) and the histological scores (E) are depicted. Error bars show SEM. Significance were determined by using either two-way ANOVA with Bonferroni corrections (A) or Mann-Whitney test as follow *p≤0.05, **p≤0.01. Scale bar represents 100µm. Results are representative of 3 independent experiments.

Figure 2: Effective horizontal transmission of the protective effect induced by apigenin. Mice were treated with apigenin at day 20, 17, 14, 10, 7 and 3 before induction of colitis by administration of 2% DSS (w/v). Mice were either single-housed or co-housed during experiment. (A) Body weight loss, (B) disease activity index, (C) colon length, (D) representative H&E stained colonic sections and (E) histological score are presented (N=4). Error bars show SEM. *p≤0.05, **p≤0.01. Scale bar represents 100µm. Results are representative of 2 independent experiments.

Figure 3: Apigenin shapes the composition of the gut microbiota through Nlrp6 activation. (A) Principal coordinate analysis of fecal bacterial communities profiled from wild-type and *Nlrp6*$^{-/-}$ mice that were treated or not with apigenin over a 3-week period. Principal coordinates were calculated on non-abundance based Jaccard distances representing community composition of compared samples. Black and white symbols represent wild-

type and *Nlrp6*$^{-/-}$ mice respectively. (B) Analysis of differences in the microbial taxa between apigenin treated and untreated wild type animals using Lefse (linear discriminant analysis [LDA] coupled with effect size measurements). Only bacterial taxa reaching LDA threshold of 2 and p value ≤ 0.05 are shown.

Figure 4: The transmissible protection driven by apigenin depends on Nlrp6 but not on Caspase-1 signaling. Single-housed mice treated over a 3-week period of apigenin treatment before being subjected to 2% DSS. Body weight loss, colon length, representative H&E stained colonic sections and colitis score are presented for (A-D) *Casp1*$^{-/-}$ mice (*Casp1*$^{-/-}$ N=3, Api-*Casp1*$^{-/-}$ N=5), (E-H) *Pycard*$^{-/-}$ mice (*Pycard*$^{-/-}$ N=4, Api-*Pycard*$^{-/-}$ N=5) and (I-L) *Nlrp6*$^{-/-}$ mice (*Nlrp6*$^{-/-}$ N=4, Api-*Nlrp6*$^{-/-}$ N=4). Error bars show SEM. *p≤0.05. Scale bar represents 100µm.

Figure 5: *Nlrp6*-deficient mice are resistant to the dominantly transmitted protection conferred by apigenin. Non-treated and apigenin-treated *Nlrp6*$^{-/-}$ mice were cohoused for 3 weeks of apigenin treatment and then subjected to DSS. (A) Body weight loss, (B) colon length, (C) representative H&E stained colonic sections and (D) colitis score are presented (*Nlrp6*$^{-/-}$ N=4, Api-*Nlrp6*$^{-/-}$ N=5). Error bars show SEM. Scale bar represents 100µm.

Figure 6: Apigenin lowers the proliferation rate of IECs in response to compositional changes in the gut microbiota downstream of Nlrp6 signalling. A. Relative expression level of Nlrp6 gene measured in the colonic tissue of single-housed wild-type mice that were treated or not with apigenin for 3 weeks and non-treated wild-type mice that were co-housed with

apigenin-treated animals (N=5). B. Representative Ki67 immunostaining in colonic tissue samples. Scale bar represents 100 µm. C. Average numbers of $Ki67^{+}$ cells per colonic crypt (non-treated N=4, apigenin-treated N=5). Black and white symbols represent WT and *Nlrp6*-deficient mice respectively. All values are mean ± SEM. *p≤0.05 **p≤0.01.

Figure 7: The protective effect of apigenin was compromised in mice that are deficient for the downstream c-type lectin reg3b. Single-housed mice treated over a 3-week period of apigenin treatment before being subjected to 2% DSS. Body weight loss, colon length, representative H&E stained colonic sections, Il1b levels in colonic explants and colitis score are presented for (A-E) wild-type mice (untreated $Reg3b^{+/+}$ N=5, Api-$Reg3b^{+/+}$ N=5) and $Reg3b^{-/-}$ mice (untreated $Reg3b^{-/-}$ N=4, Api-$Reg3b^{-/-}$ N=5),. Error bars show SEM. *p≤0.05. Scale bar represents 100µm.

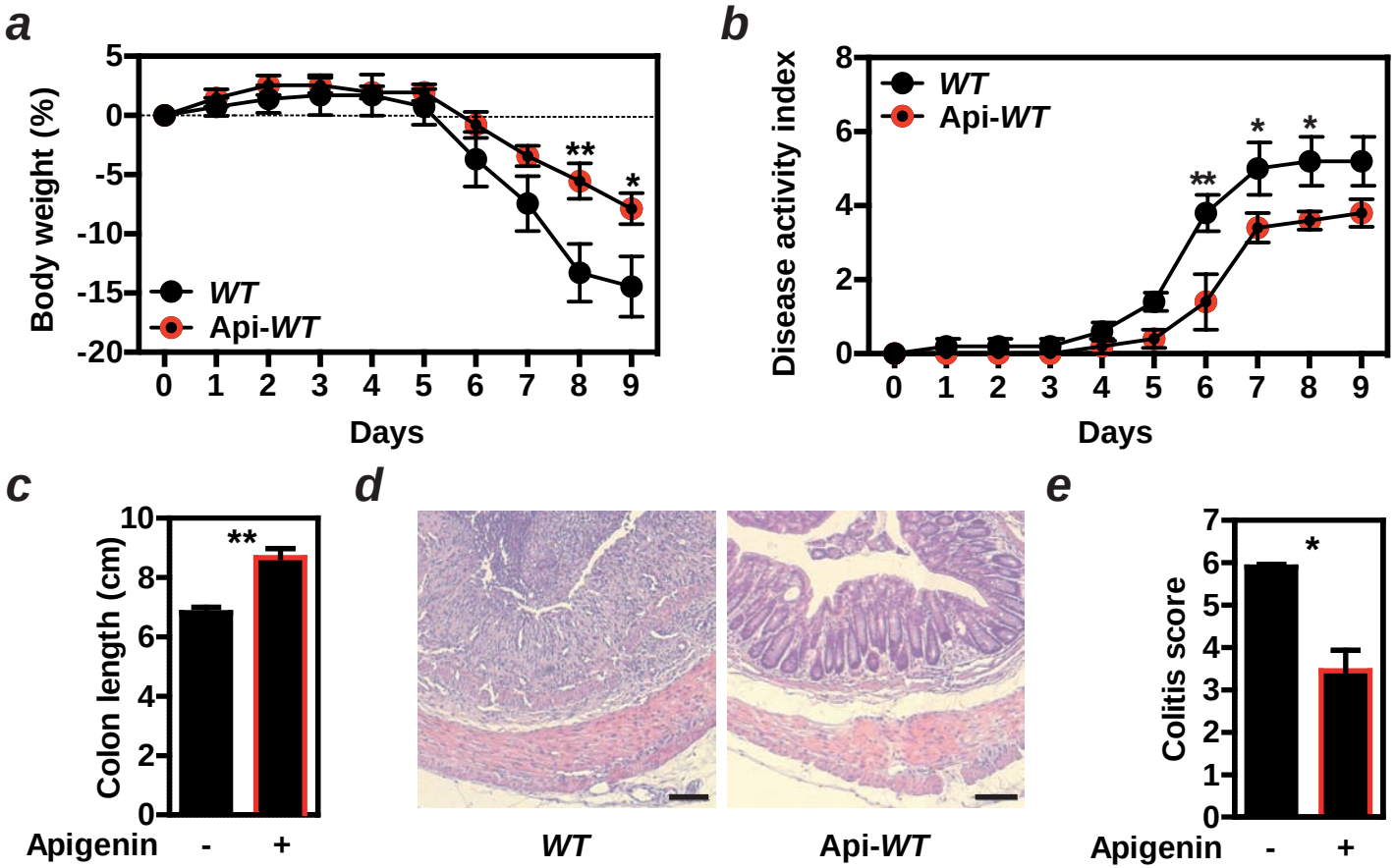
a
Body weight (%)
5
0
-5
-10
-15
-20
0 1 2 3 4 5 6 7 8 9
Days
WT
Api-WT
**
*
b
Disease activity index
8
6
4
2
0
0 1 2 3 4 5 6 7 8 9
Days
WT
Api-WT
**
*
*
c
Colon length (cm)
10
8
6
4
2
0
**
Apigenin - +
d
WT
Api-WT
e
Colitis score
7
6
5
4
3
2
1
0
*
Apigenin - +

Figure 1

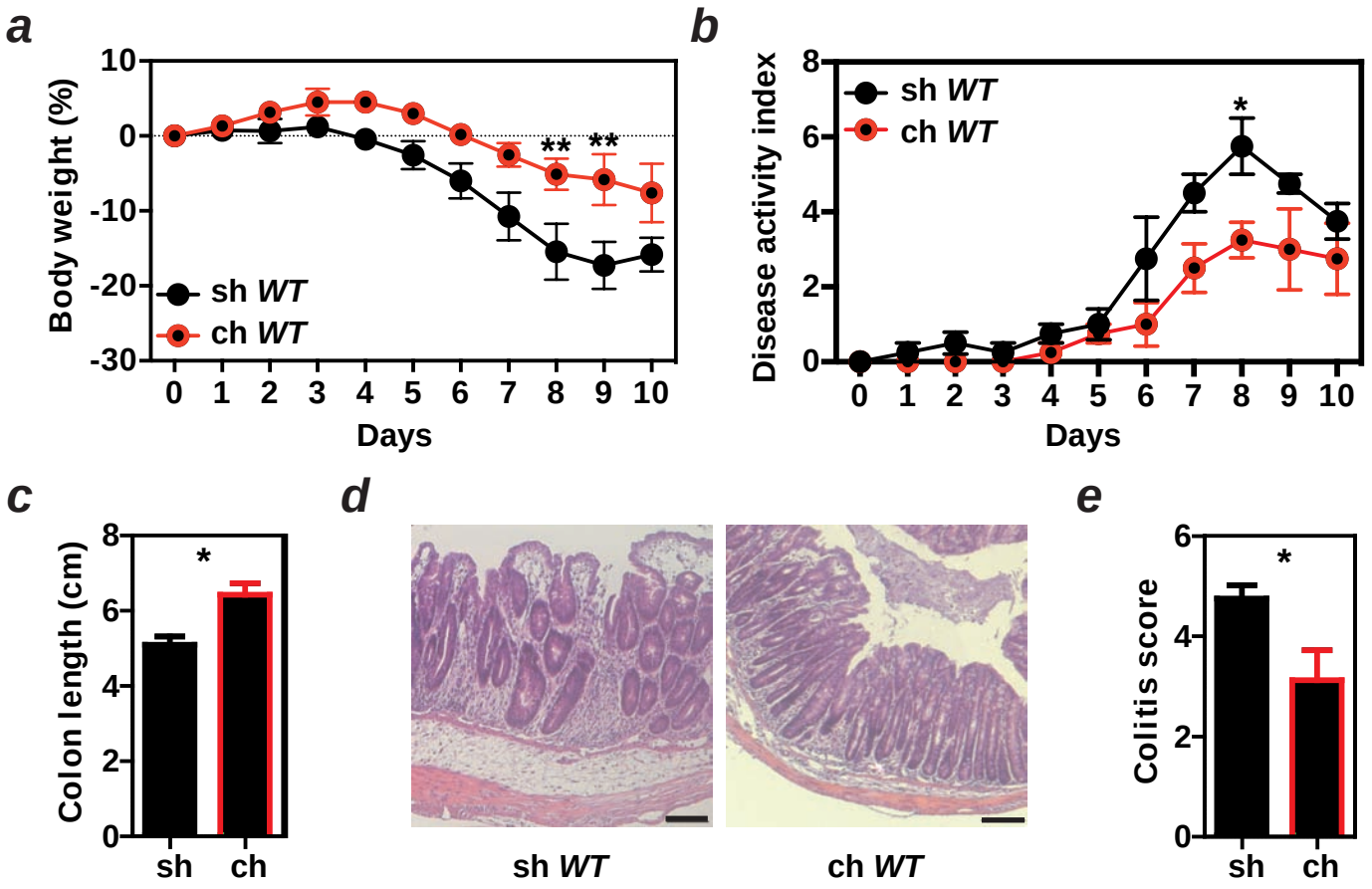
a
Body weight (%)
10
0
-10
-20
-30
0 1 2 3 4 5 6 7 8 9 10
Days
sh WT
ch WT
**
**
b
Disease activity index
8
6
4
2
0
0 1 2 3 4 5 6 7 8 9 10
Days
sh WT
ch WT
*
c
Colon length (cm)
8
6
4
2
0
sh ch
*
d
sh WT
ch WT
e
Colitis score
6
4
2
0
sh ch
*

Figure 2

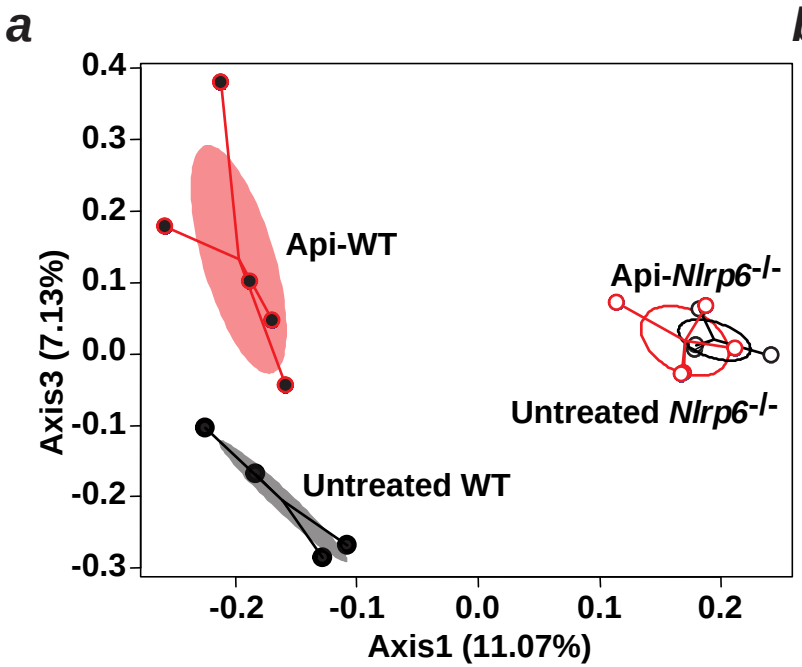
a
0.4
0.3
0.2
0.1
0.0
-0.1
-0.2
-0.3
Axis3 (7.13%)
-0.2
-0.1
0.0
0.1
0.2
Axis1 (11.07%)
Api-WT
Api-Nlrp6-/-
Untreated Nlrp6-/-
Untreated WT

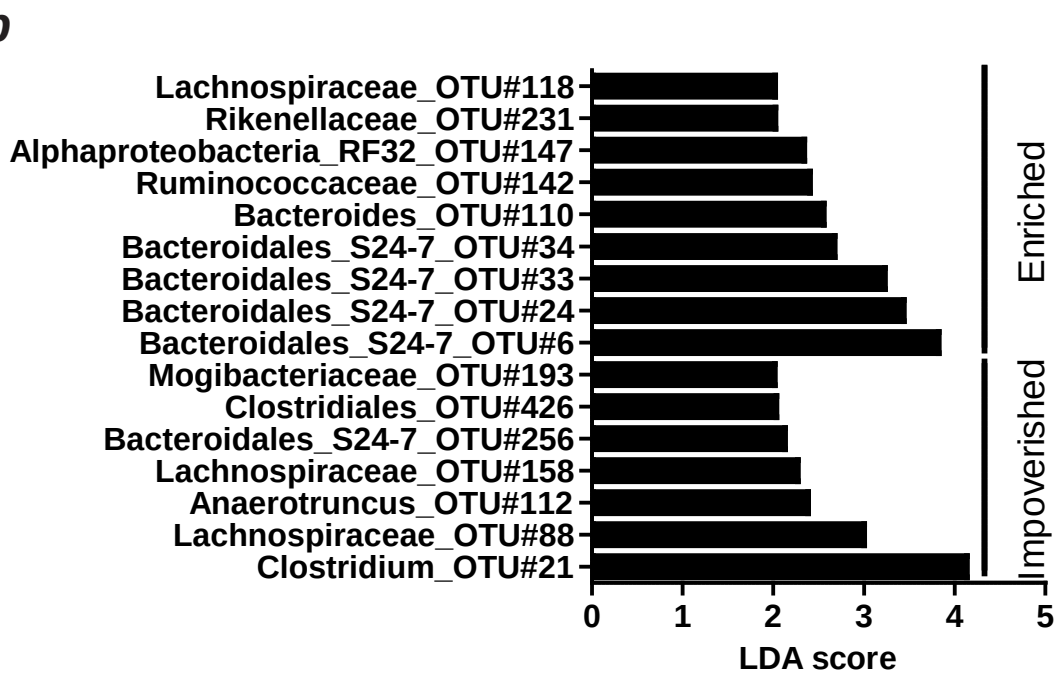
b
Lachnospiraceae_OTU#118
Rikenellaceae_OTU#231
Alphaproteobacteria_RF32_OTU#147
Ruminococcaceae_OTU#142
Bacteroides_OTU#110
Bacteroidales_S24-7_OTU#34
Bacteroidales_S24-7_OTU#33
Bacteroidales_S24-7_OTU#24
Bacteroidales_S24-7_OTU#6
Mogibacteriaceae_OTU#193
Clostridiales_OTU#426
Bacteroidales_S24-7_OTU#256
Lachnospiraceae_OTU#158
Anaerotruncus_OTU#112
Lachnospiraceae_OTU#88
Clostridium_OTU#21
Enriched
Impoverished
0
1
2
3
4
5
LDA score

Figure 3

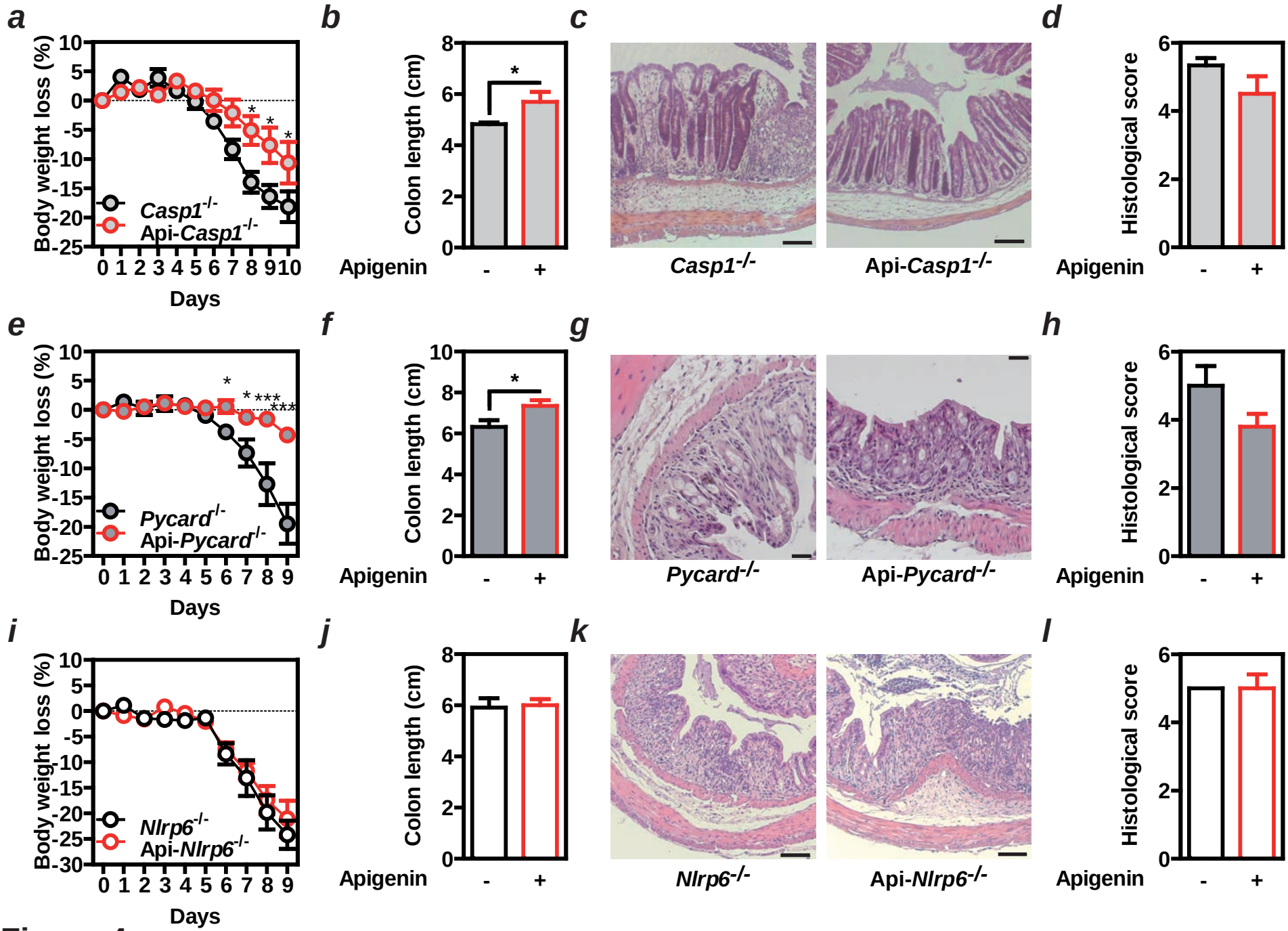
a
Body weight loss (%)
Days
Casp1-/-
Api-Casp1-/-
b
Colon length (cm)
Apigenin
c
Casp1-/-
Api-Casp1-/-
d
Histological score
Apigenin
e
Body weight loss (%)
Days
Pycard-/-
Api-Pycard-/-
f
Colon length (cm)
Apigenin
g
Pycard-/-
Api-Pycard-/-
h
Histological score
Apigenin
i
Body weight loss (%)
Days
Nlrp6-/-
Api-Nlrp6-/-
j
Colon length (cm)
Apigenin
k
Nlrp6-/-
Api-Nlrp6-/-
l
Histological score
Apigenin

Figure 4

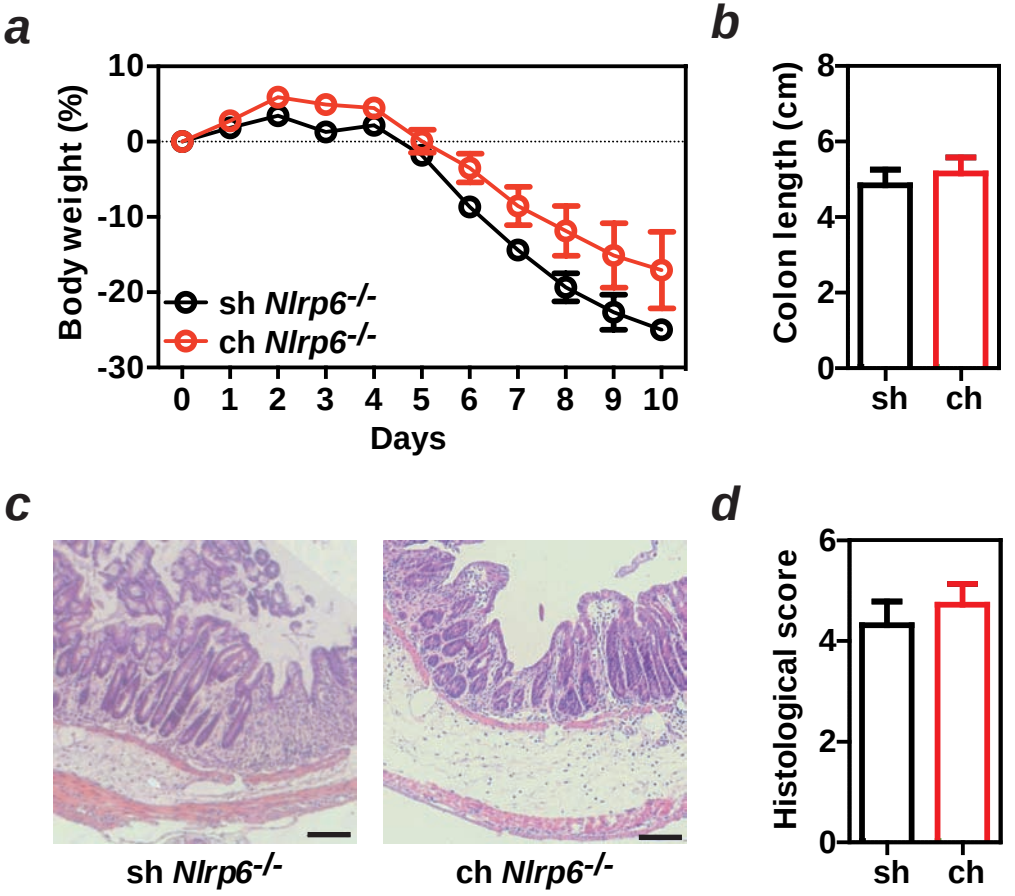
a
b
c
d
Body weight (%)
10
0
-10
-20
-30
0 1 2 3 4 5 6 7 8 9 10
Days
sh Nlrp6-/-
ch Nlrp6-/-
Colon length (cm)
8
6
4
2
0
sh
ch
Histological score
6
4
2
0
sh
ch
sh Nlrp6-/-
ch Nlrp6-/-

Figure 5

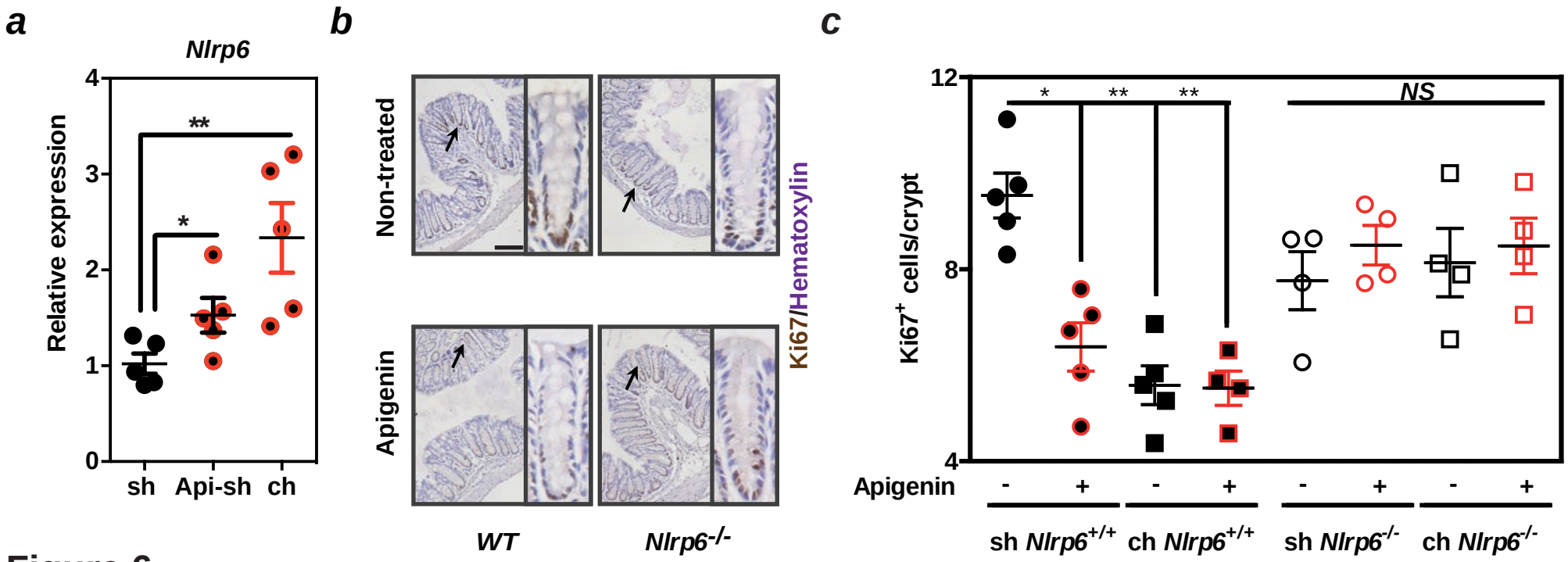
a
Nlrp6
Relative expression
4
3
2
1
0
**
*
sh
Api-sh
ch
b
Non-treated
Apigenin
Ki67/Hematoxylin
WT
Nlrp6-/-
c
Ki67+ cells/crypt
12
8
4
*
**
**
NS
Apigenin
-
+
-
+
-
+
-
+
sh Nlrp6+/+
ch Nlrp6+/+
sh Nlrp6-/-
ch Nlrp6-/-

Figure 6

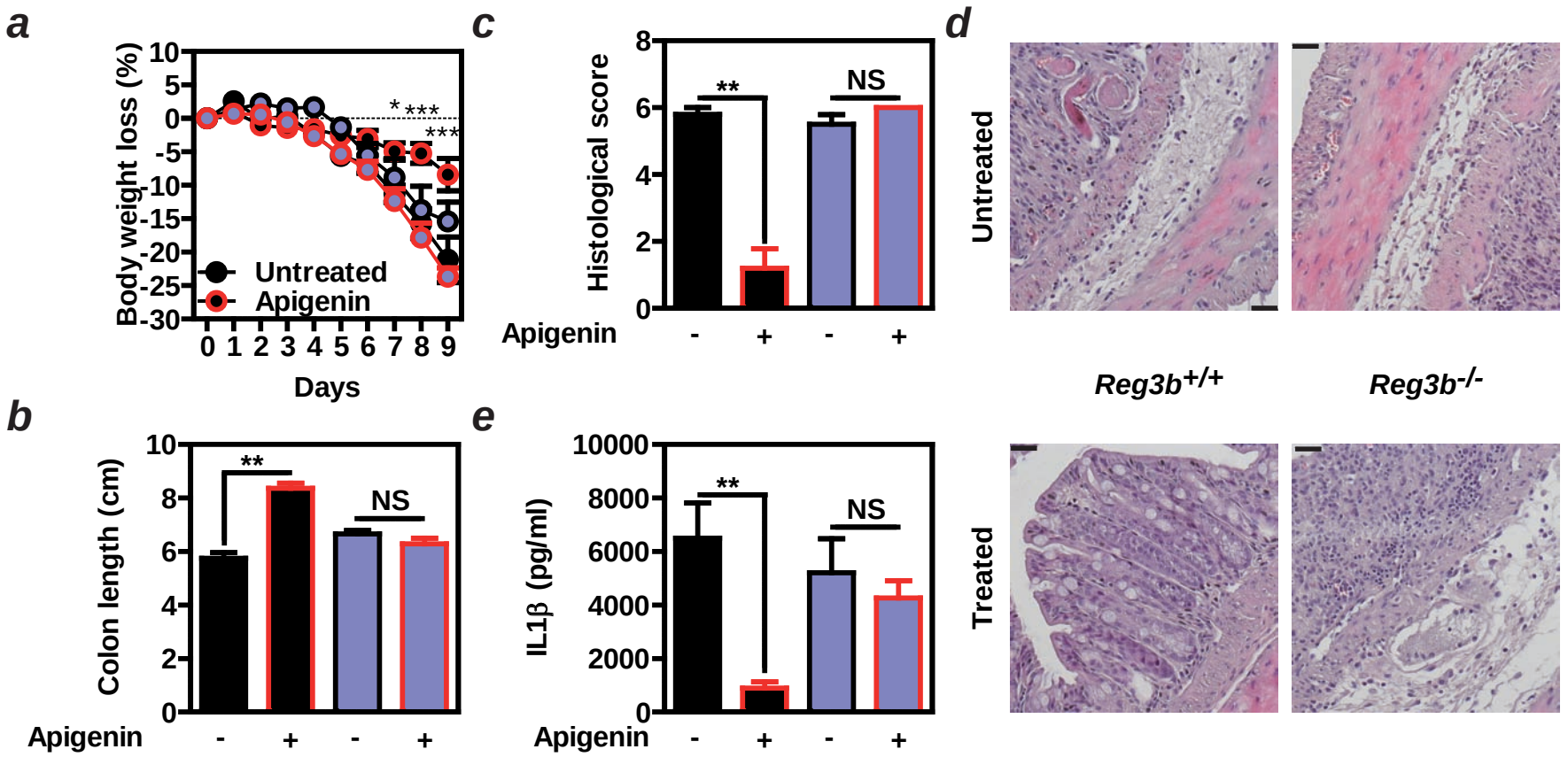
a
Body weight loss (%)
10
5
0
-5
-10
-15
-20
-25
-30
0 1 2 3 4 5 6 7 8 9
Days
Untreated
Apigenin
*
***
***
c
Histological score
8
6
4
2
0
**
NS
Apigenin
-
+
-
+
d
Untreated
Treated
Reg3b+/+
Reg3b-/-
b
Colon length (cm)
10
8
6
4
2
0
**
NS
Apigenin
-
+
-
+
e
IL1β (pg/ml)
10000
8000
6000
4000
2000
0
**
NS
Apigenin
-
+
-
+

Figure 7

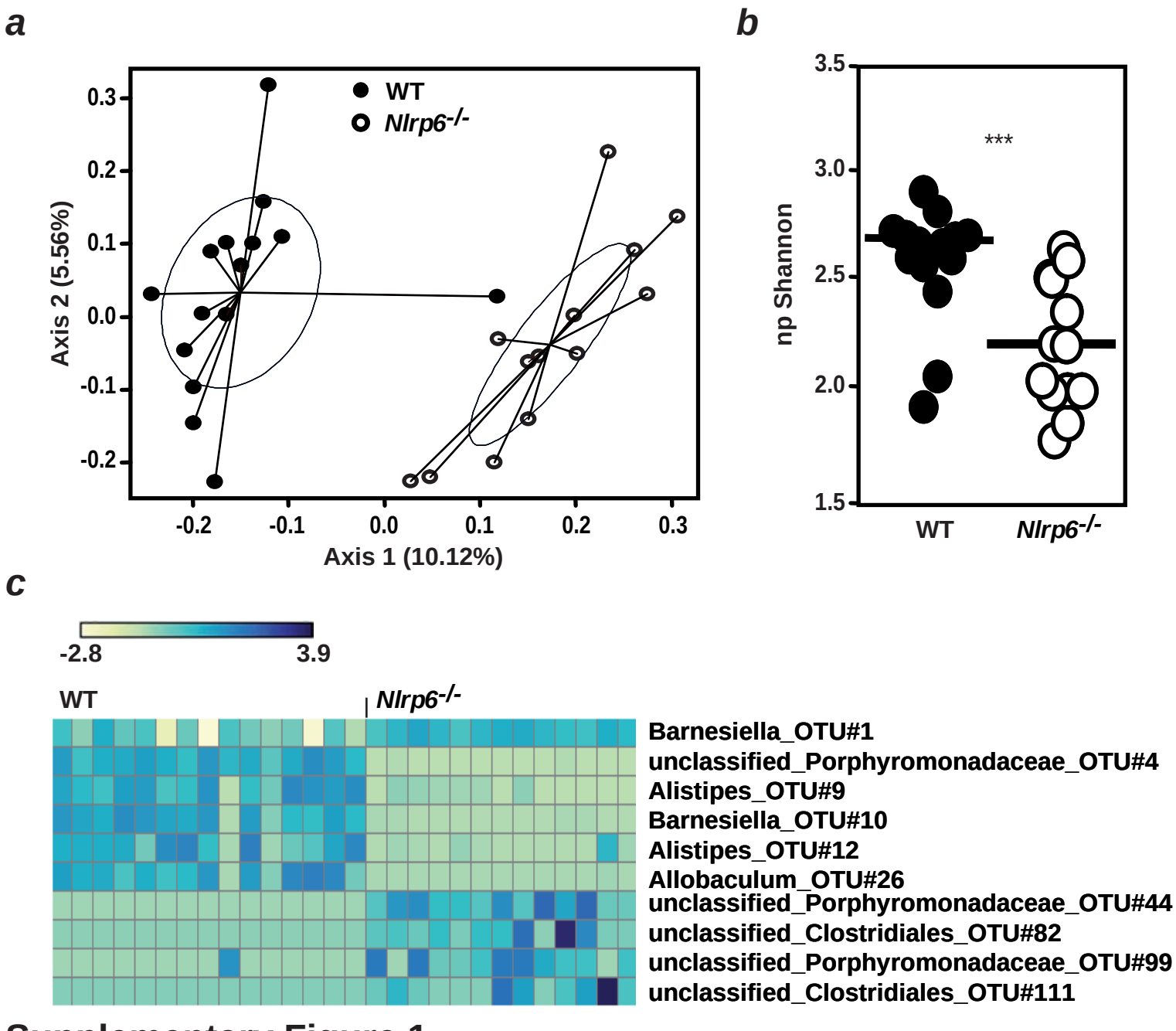

Supplementary Figure 1

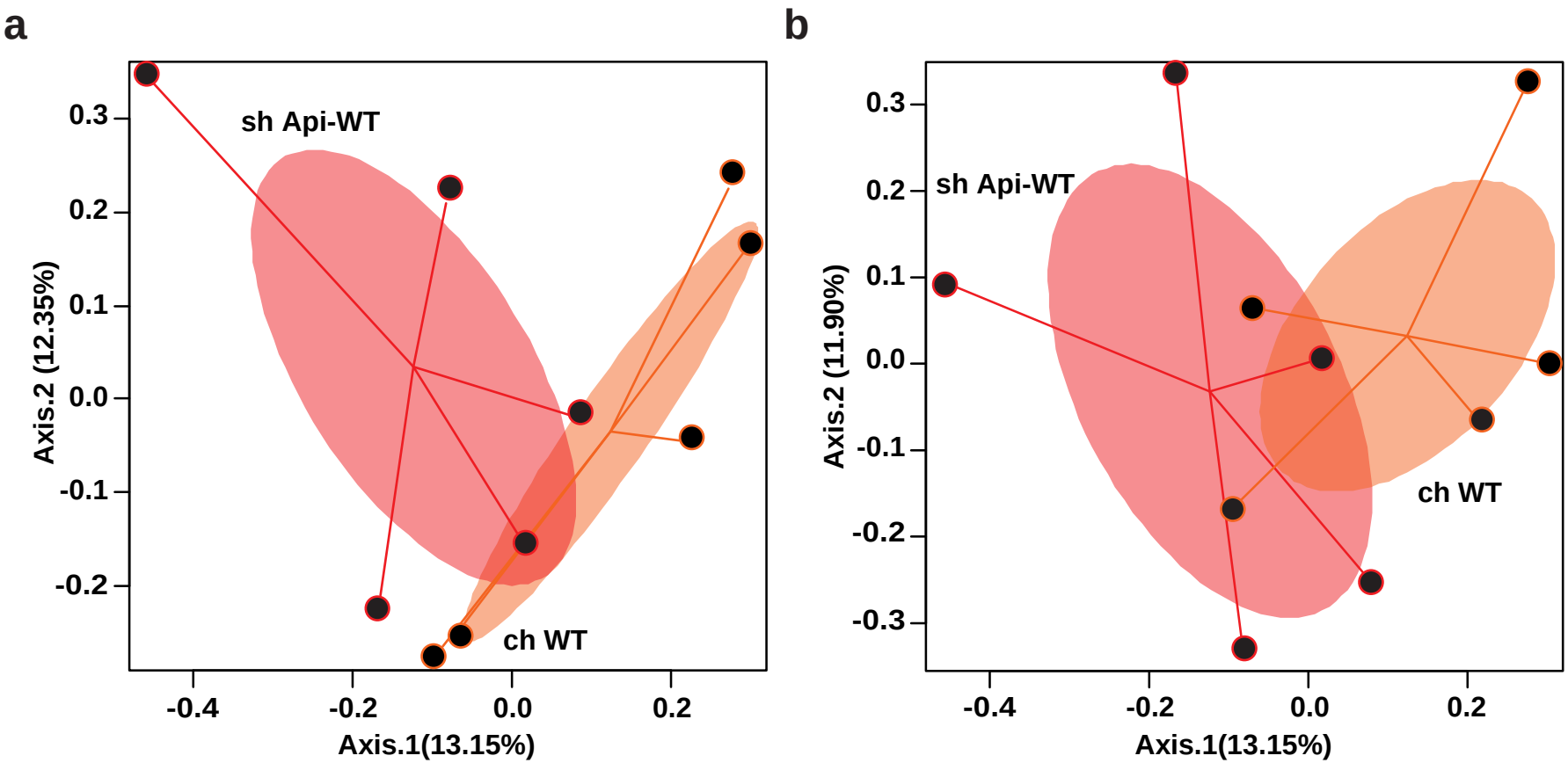

Supplementary figure 2

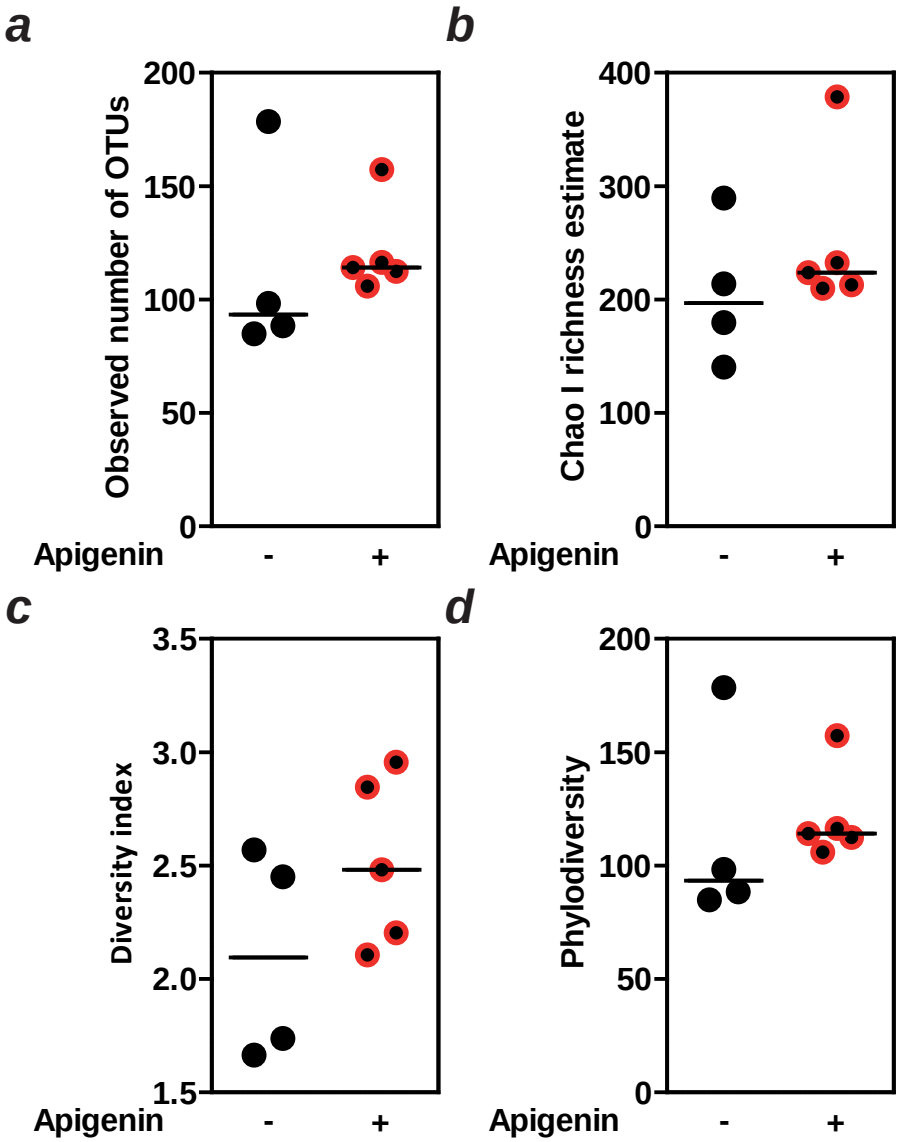

Supplementary figure 3

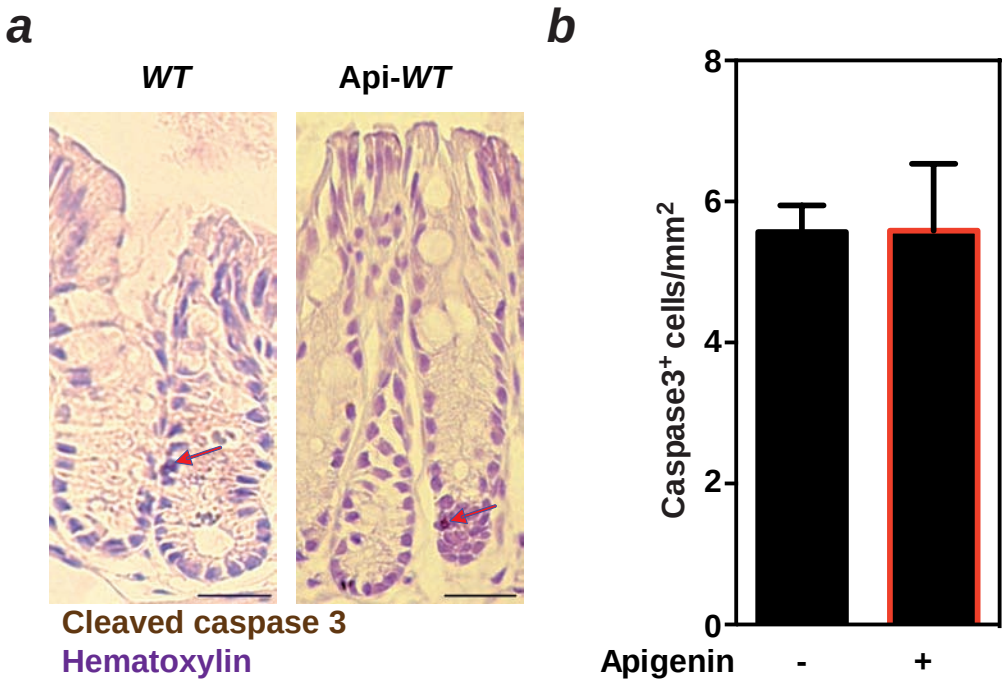

Supplementary figure 4

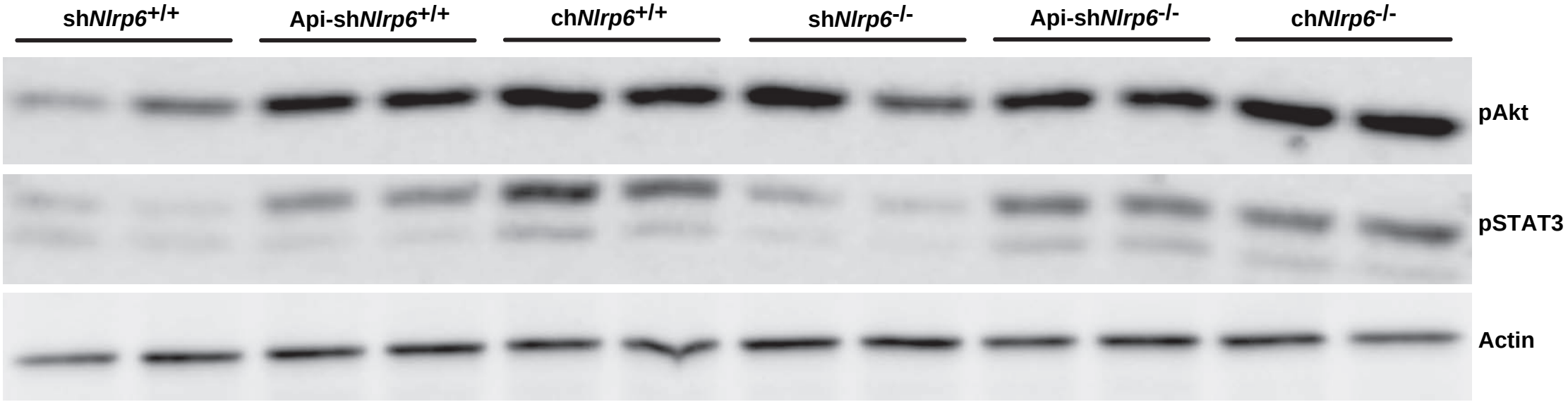

Supplementary figure 5

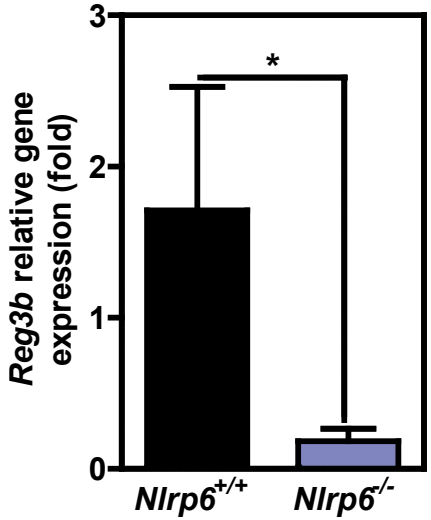

Supplementary figure 6